LIMNOLOGY
and
OCEANOGRAPHY: METHODS

Limnol. Oceanogr.: Methods 10, 2012, 304–316

Oxygen optodes as fast sensors for eddy correlation measurements in aquatic systems

Lindsay Chipman[1], Markus Huettel[1], Peter Berg[2], Volker Meyer[3], Ingo Klimant[4], Ronnie Glud[5,6], and Frank Wenzhoefer[3,7]*

[1]Florida State University, Department of Earth, Ocean and Atmospheric Science, Tallahassee, FL 32306
[2]Department of Environmental Sciences, University of Virginia, Charlottesville, VA, USA
[3]Max Planck Institute for Marine Microbiology, Bremen, Germany
[4]Graz University of Technology, Graz, Austria
[5]Institute of Biology, University of Southern Denmark (Nordic Center for Earth Evolution), Odense, Denmark
[6]Scottish Association for Marine Science, Dunstaffnage Marine Laboratory, PA37 1QA, Dunbeg, Scotland
[7]HGF MPG Joint Research Group Deep Sea Ecology and Technology, Alfred Wegener Institute for Marine and Polar Research, Bremerhaven, Germany

Abstract

The aquatic eddy-correlation technique can be used to noninvasively determine the oxygen exchange across the sediment-water interface by analyzing the covariance of vertical flow velocity and oxygen concentration in a small measuring volume above the sea bed. The method requires fast sensors that can follow the rapid changes in flow and the oxygen transported by this flow to calculate the momentary advective flux driven by turbulent motions. In this article, we demonstrate that fast optical oxygen sensors, known as optodes, represent a good alternative to the traditional Clark-type electrochemical microelectrodes for such measurements. Optodes have the advantage over microelectrodes of being insensitive to flow, less susceptible to signal drift, more durable under typical field conditions, less expensive, and repairable. Comparisons of the response times of optodes and microelectrodes to rapid oxygen changes showed that optimized optodes had the same response time (162 ± 66 ms) as the microelectrodes (160 ± 57 ms) and were fast enough to capture the oxygen fluctuations that are relevant for the eddy correlation flux calculations. Side by side comparisons of benthic O_2 flux data collected with microelectrode-based eddy correlation instruments and optode-based eddy correlation instruments in freshwater and marine environments showed no significant differences between the measured fluxes. The optodes allow the development of more user-friendly eddy correlation instruments that combine the advantages of noninvasive measurements and integration of fluxes over a large footprint area, using a relatively rugged and less expensive sensor.

Oxygen flux measurements at the seafloor are fundamental for the understanding of respiration and oxidation processes and the global cycling of matter (Jahnke and Craven 1995; Jahnke 1996). Where anaerobic mineralization products are fully oxidized within the sea bed, benthic oxygen consumption reflects the mineralization of organic carbon (Canfield et al. 1993), and oxygen flux can be used as proxy for assessing carbon cycling rates (Glud 2008). Oxygen is transported across the sediment-water interface mainly by molecular diffusion, bioturbation, bioirrigation, and current- or wave-driven advective exchange (Ziebis et al. 1996). In shallow waters, photosynthesis of benthic phototrophic organisms (e.g., microalgae, cyanobacteria) produces oxygen in the uppermost surface layer of the sediment (Cahoon 1999). Interfacial transport and photosynthesis control oxygen availability to sedimentary oxidation processes and benthic communities, thereby affecting sediment oxygen consumption and fluxes. Because bottom flows and light can influence oxygen flux, it is preferable to measure benthic fluxes without disturbing boundary layer flows and the light field at the sea floor. Tradi-

*Corresponding author: E-mail: mhuettel@fsu.edu

Acknowledgments

We thank Dave Oliff (FSU Oceanography) for technical support and Anni Glud for manufacturing the fast responding microelectrodes. Michael Santema, Chiu Cheng, John Kaba, Lee Russell, and Chris Hagan (all FSU/EOAS) helped during instrument deployments in the field; funding for this project was provided by NSF Grants OCE-536431 and OCE-0758446.

DOI 10.4319/lom.2012.10.304

tional flux measuring techniques, such as benthic chamber incubations and the measurement of oxygen concentration profiles across the sediment water interface, interfere with the natural light and flow regime and cannot fully capture the natural temporal fluctuations.

The eddy correlation method was first developed to measure atmospheric fluxes (Swinbank 1951) and has recently been successfully used to measure oxygen fluxes in both marine and freshwater environments (Berg et al. 2003, 2009; Kuwae et al. 2006; Berg and Huettel 2008; Brand et al. 2008; McGinnis et al. 2008; Reimers et al. 2012). The eddy correlation method has several advantages over traditional flux-measuring techniques including the integration over a larger sediment surface area (Berg et al. 2007), minimal interference with in situ conditions (Berg et al. 2003, 2009), and the ability to measure over substrates that do not permit chamber deployments or measurements of oxygen concentration profiles, e.g., dense seagrass beds and hard bottoms (Glud et al. 2010; Hume et al. 2011).

The method can produce largely unbiased flux data and is based on the assumption that oxygen traveling toward or away from the sediment is transported by turbulent motion. Vertical oxygen flux can be calculated as the average over a period, significantly longer than the time scale of turbulent fluctuations and variations in BBL structure:

$$\overline{\text{Flux}} = \overline{u'_z C'} \quad (1)$$

where (u'_z) is the fluctuating component of the vertical velocity and (C') the fluctuating component of the oxygen concentration (Reynolds 1895; Berg et al. 2003).

The instrumentation for aquatic eddy measurements has, until now, consisted of a fast Clark-type oxygen microelectrode (Revsbech and Ward 1983; Gundersen et al. 1998) and a Nortek acoustic Doppler velocimeter (ADV). Oxygen microelectrodes were introduced to aquatic science in the early eighties (Revsbech et al. 1979; Revsbech et al. 1980) and are now widely used for the investigation of a large variety of physical, biological, and chemical processes in aquatic environments. They allow measurements at high spatial (µm-scale) and temporal (ms-scale) resolution, and thus, are able to resolve fine scale and highly dynamic processes (Revsbech 1989; Revsbech and Jørgensen 1986). These characteristics make them very suitable for eddy correlation measurements. Their key problems are their susceptibility to occasional signal drift, their oxygen consumption that can cause stirring sensitivity (Gundersen et al. 1998), their fragility, and their technical complexity that is reflected in the time-consuming manufacturing process and ensuing high sensor cost. Optical fiber sensors, called optodes or optrodes, have been developed for oxygen measurements (Glud et al. 1999; Holst et al. 1997; Holst et al. 1998; Klimant et al. 1995) and would be a viable replacement to the microelectrode provided they have a sufficiently fast response time and have the adequate sensitivity. The sensing tip of an oxygen optode is coated with a fluorophore that changes its fluorescence characteristics when exposed to oxygen, i.e., oxygen acts as a dynamic fluorescence quencher, decreasing the fluorescence quantum yield of the fluorophore (Kautsky 1939). The relationship between oxygen concentration and fluorescence intensity is non-linear and can be described by the Stern-Volmer equation:

$$I_0 / I = 1 - K_{sv} \times C \quad (2)$$

where I and I_0 and are the fluorescence intensities in the presence and absence of oxygen, respectively, K_{sv} is a constant expressing the quenching efficiency, and C is the oxygen concentration (Stern and Volmer 1919). This equation is only valid for ideal systems such as the quenching of dilute solutions of fluorophores. Klimant et al. (1995) and Glud et al. (1996) showed that the response of most optodes can be described by a slightly modified Stern-Volmer equation

$$I = I_0 \left[\alpha + (1-\alpha) \left(\frac{1}{1 + K_{SV} C} \right) \right] \quad (3)$$

where α is the nonquenchable fraction of the fluorescence.

Optodes have the advantages over microelectrodes of being less susceptible to signal drift, more durable in the field conditions to which the system is typically exposed, less expensive to fabricate, and repairable (i.e., a broken tip can be retapered and recoated). While microelectrodes consume small amounts of oxygen when measuring (Gundersen et al. 1998), optodes are in a thermo-dynamical equilibrium with their environment, and no oxygen is consumed during the measurement. In contrast to the microelectrode, the optode signal therefore is independent of flow. With these advantages, optodes could be the preferable sensor for eddy correlation measurements provided that the optodes are fast enough to capture the oxygen fluctuations that carry the flux signal. Here we introduce a sensor system based on optodes and present laboratory and field measurements that investigate the feasibility of optode eddy correlation measurements in freshwater and marine environments.

Materials and procedures

Instrumentation

1) Optode-based eddy correlation oxygen flux system (Fig. 1)

The fast optical oxygen meter integrated in this system consists of the optode sensor and a custom-made electronics board that is mounted with a 18V rechargeable battery in an underwater housing. The custom-made optodes (Klimant lab) were fabricated using a 100/140 µm multimode glass fiber cable with a standard connector (ST-type). At the fiber end, the cladding (protective plastic mantle) was removed and the exposed fiber was passed through the cylinder of a plastic 1 mL syringe and the attached hypodermic needle (0.7 mm inner diameter). The

Fig.1. (A) Eddy correlation instrument with oxygen optode. (B) ADV sensor head and two optodes. (C) Optodes housed in 1 mL syringe. The dark spot at the end of the glass fiber protruding from the needle is the sensing dye. The dark line parallel to fiber is the shadow of the fiber.

fiber then was secured to the syringe plunger such that the tip of the fiber could be moved out of the needle to a length of approximately 5 mm. To minimize the response time of the optode, the fiber tip was tapered by hydrofluoric acid-edging to a diameter of < 50 µm. This tip was coated with the oxygen-sensitive dye with the fluorophore ruthenium (II)-tris-4, 7-diphenyl-1, 10-phenanthroline perchlorate. This fluorophore absorbs blue light at 450 nm and emits a strong red luminescence with a wavelength maximum at 610 nm (Gruber et al. 1993). The thickness of the dye coating was reduced to a minimum (~20 µm), to optimize the response time. The optimal thickness of the sensing chemistry is a trade-off between fast response time and signal size (amplitude). A thinner sensor tip with thinner dye coating allows a faster response time because the diffusive boundary layer around the tip is less developed and the diffusion of oxygen to the sensor dye on the tip is faster. However, the amplitude of the signal is reduced with reduced dye thickness. Because larger signal amplitudes are associated with less signal noise, the sensor thickness must be chosen to optimize response time while measuring with an acceptable signal noise.

The custom-made analog board (Fig. 2), connected via a 15VDC/12VDC converter to the battery, provides the excitation light for the optode and processes the fluorescence signal. A driver unit on the board operates a diode (Nichia, 475 nm) that emits blue light through a blue bandpass filter (475 nm, bandwidth 50 nm), which cleans the diode output. The driver unit permits adjustment of the intensity of the excitation light allowing selection of the optimal setting for the sensor in use. This excitation light is modulated at 4 kHz to distinguish between the fluorescence light emitted by the sensor dye and ambient light. A 50:50 X-coupler (Gould) splits the light beam into two equal beams. One of the beams is led via a fiber and a Lee-filter (450 nm) onto a pin-diode that quantifies the excitation light and provides a control signal. The latter is used to regulate the current for the light-emitting diode, thereby preventing fluctuations in light intensity that could be erroneously interpreted as changes in oxygen concentration. The light of the second beam is guided via a 100/140 µm multimode glass fiber and a pressure-resistant underwater housing penetrator to the tip of the optode, where it excites the oxygen-sensitive sensor dye. The fluorescence emission of the sensor dye, which increases with decreasing oxygen concentration in the water, is returned through the same fiber and the X-coupler to a Schott OG 590 filter that only permits the fluorescence emission wavelength to pass through to the photomultiplier (Hamamatsu). The photomultiplier translates changes in the photon flux into a signal of voltage changes. A high-pass circuit separates noise caused by ambient light from the modulated voltage signal. Then the signal is rectified and amplified through a circuit that allows change in the gain by a factor of 1 to10, so that the output voltage range can be optimized to match the voltage range of the analog-digital converter of the ADV data logger. In laboratory tests, the accuracy of the calibrated system was ± 1% of air saturation or approximately ± 2.5 µmol L^{-1}.

For some of the tests, a second commercially available optode system, the Presens Microx TX3, was mounted next to the custom board in the underwater cylinder. The Microx TX3 determines oxygen concentrations based on fluorescence lifetime measurements at a rate of 3 to 4 s^{-1}. The optodes attached to the Microx TX3 were those supplied by the manufacturer of the instrument (Presens), and the accuracy of the system is also ± 1% of air saturation.

In both cases, the optode signals were recorded by the data logger of the Nortek Vector acoustic Doppler velocimeter (ADV) that was used for the flow measurements. The ADV measures the magnitude of the three flow velocity components using the Doppler effect. The accuracy of the system is ± 0.5% of the measured value (e.g., 1 mm s^{-1} at a flow of 20 cm s^{-1}). The simultaneous recording of oxygen concentrations and flow velocities at a rate of 64 s^{-1} by the same data logger allowed the oxygen data to be related directly to the respective flow data.

The aluminum underwater housing with the oxygen meters and the Nortek Vector were mounted on a small stainless steel tripod (120 cm width, 80 cm height) with thin legs (1.2 cm diameter) to minimize interference with bottom water

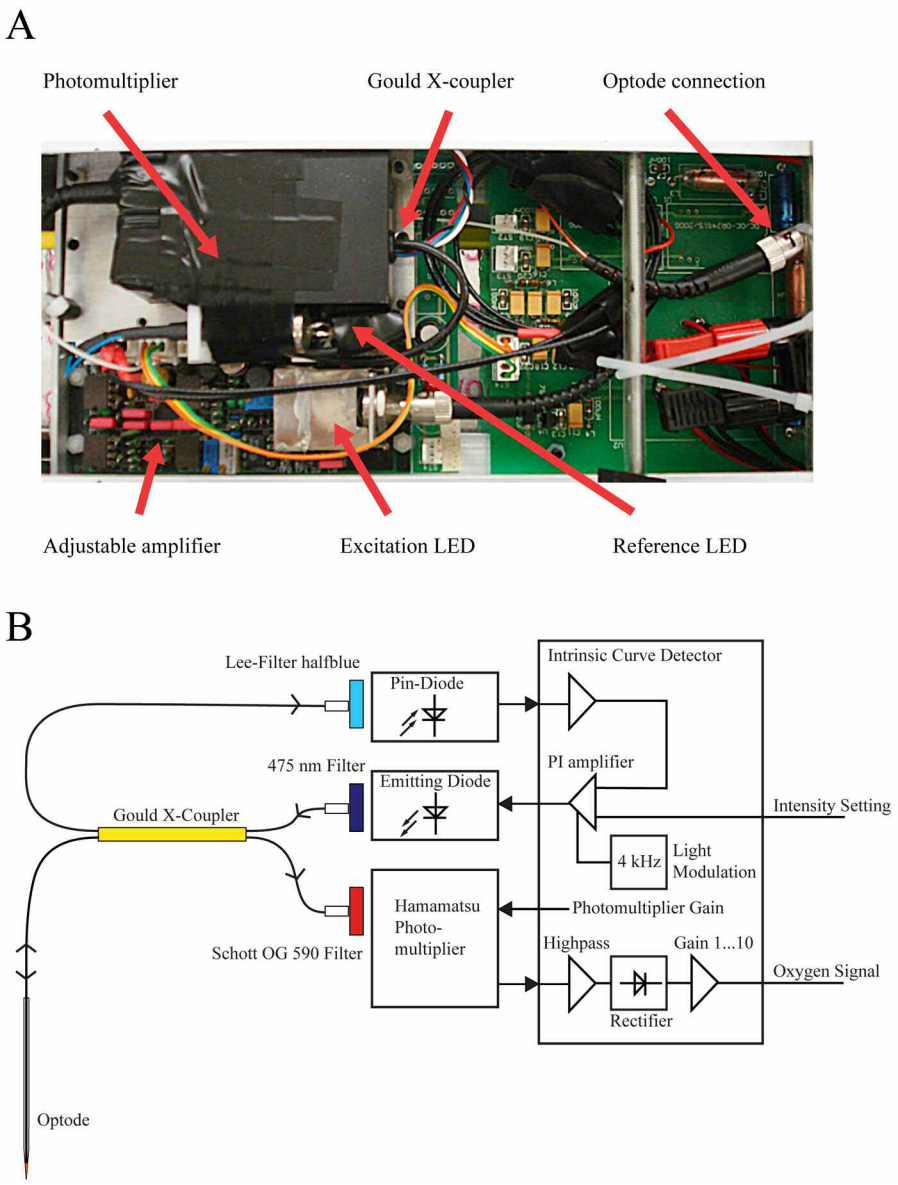

Fig. 2. (A) The custom analogue optode board. (B) Electronic schematic of the board showing main components, connections, and signal passage. For further explanation, see text.

flow (Fig. 1). The fiber optic cables attached to the oxygen meters extended through a pressure-proof feed-through from the aluminum housing and ended in standard ST-connectors. These were linked via fiber couplers to the ST-connectors of the optodes. The couplers and ST-connectors were encased in a sealed PVC tubing protecting them from water. An adjustable stainless steel rod (0.6 cm diameter) carried the optode(s) and was used to place the tips of the optode(s) directly at the lower edge of the ADV measuring volume (14 mm height, 14 mm diameter), which is located at 157 mm (center) below the sensor head. The legs of the tripod were adjusted such that this measuring volume was located at 12-15 cm above the sediment-water interface. At this measuring height, the footprint (area contributing to the flux) of the eddy correlation measurements is approximately 1 m wide and ranges between 12 and 65 m length depending on sediment roughness (Berg et al. 2007). Our instrument had a depth rating of 300 m.

2) Microelectrode-based eddy correlation oxygen flux system

In laboratory and field tests, the performance of the optode eddy correlation system was compared with that of a traditional microelectrode-based eddy correlation system as described and shown in Berg and Huettel (2008). This system used a fast-response oxygen microelectrode connected to a custom-built picoampere meter. The Clark-type microelectrode equipped with a guard cathode was optimized through

a small tip opening of < 2 µm, and optimal distance between tip and the measuring cathode to ensure low stirring sensitivity but fast response time (Gundersen et al. 1998). This microelectrode eddy correlation instrument also used a Nortek Vector acoustic doppler velocimeter for the flow measurements. The ADV logger collected velocity and oxygen data simultaneously at 64 s^{-1}. The accuracy of the oxygen measurements was ± 0.2% of air saturation or approximately ± 0.5 µmol L^{-1}.

3) Instruction for setting up and deployments of an optode-based eddy correlation system

After setting up the optode-based system as decribed above, the ADV and its data logger are started and the power is switched on for the optode electronics, which initiates the collection of optode oxygen data on the ADV data logger. Before initiating the measurements, the optode is calibrated by successively submerging the tip in oxygen-saturated and oxygen-free water contained in small calibration containers kept at in situ temperature—this procedure is repeated multiple times. This calibration record is stored in the same data file as the deployment data. After calibration, the instrument is placed on a flat, horizontal area of the seabed. If the instrument is placed by divers, the optode can be retracted into the hypodermic needle for protection during deployment, and after positioning of the instrument, the diver pushes the plunger of the syringe containing the optode, which moves the optode tip out of the needle. When the measurements are completed, the initial calibration routine is repeated and the data are stored in the measuring file. To check sensor calibration during the field deployments, all in-situ data sets are also calibrated against reference oxygen values measured continuously during the deployment with a calibrated commercially available macro optode (Hach LDO101 IntelliCAL Rugged Dissolved Oxygen Probe) positioned near the ADV. After completion of the measurements, the data file is downloaded from the ADV logger to a computer and extracted using the Vector software package. The resulting data files are then processed in data analysis programs. The microelectrode-based eddy instrument was deployed by the same procedure except that an underwater housing containing a pico-amperemeter instead of the optode electronics was mounted to the support frame.

Data analysis

Oxygen and flow data sets are despiked and reduced by averaging to 16 s^{-1} to decrease signal noise. Outlying peak values are identified by looking carefully through each burst of the data set for noticeable spikes in the oxygen and velocity signals, and concurrent irregularities in the cumulative flux (e.g., jumps, noise). If the irregularity is caused by a single or few-points spike, this data point(s) is replaced with the avg ± 10 data points. If there are numerous spikes or noise in the signal, the time interval for which the noise occurred is removed. Oxygen fluxes are calculated by multiplying the instantaneous values of the fluctuating components of the oxygen concentration, C', with the associated instantaneous values of the fluctuating components of vertical flow velocity, u'_z, and summing the resulting products over the selected time interval(s). The fluctuating components of the oxygen concentration (C') and vertical flow velocity (u'_z) are defined as:

$$C' = C - \overline{C} \tag{4}$$

$$u'_z = u_z - \overline{u}_z \tag{5}$$

where C and u_z are the concentration and vertical velocity data values, $\overline{C}$ and $\overline{u}_z$ are the mean concentration and mean vertical velocity (Berg et al. 2003, 2009). In the calculation of the eddy flux, it is assumed that the mean of the vertical velocity (u_z) is zero. However, due to natural topography, it is often not possible to position the ADV so that the z-direction is oriented exactly perpendicular to the sediment to fulfill this criterion; in these cases a correction must be made. This is done by rotating the measured 3-D velocity field in each burst so that the means of u_z and u_y equal zero. As the mean oxygen concentration and mean vertical flow velocity may change over time, a definition of these variables is necessary to account for such temporal changes. Several common definitions exist for these means that are used to remove nonturbulent variations from the measured data. These are mean removal, linear detrending, and running averaging (Lee et al. 2004; Berg et al. 2003). Which one to use, depends on the field situation. At our study sites, linear detrending and running averaging produced very similar results, and for the flux calculations presented in this article, linear detrending was used to define the mean oxygen concentration and mean vertical velocity (software "EddyFlux," Berg lab). To determine the frequency range of eddies contributing to the flux, and to assess whether the optodes were able to adequately capture all fluctuations in oxygen concentration that contributed to the flux, cumulative co-spectra of the oxygen concentration and vertical velocity were evaluated (Smith 1997; Berg et al. 2003; Lee et al. 2004; Lorrai et al. 2010). For example, whether all eddies contributing to the flux were recorded, can be assessed by analyzing, in particular, the high frequency sections of the cumulative cospectra (Horst 1997; Horst and Lenschow 2009). Differences in the high frequency end of cospectra that are calculated from data collected by both fast electrodes and optodes show whether the optode can capture the high frequency components of the flux. Obviously, is it as important to have flux-contributing eddies with low frequencies well-represented in the data. The lengths of individual data bursts and the size of the time averaging window, if running averaging is used to define the means, are important variables in that respect. At some sites, it is not trivial to make these choices, as discussed in detail by Reimers et al. (2012). In our measurements, the co-spectra revealed that flux-contributions at high frequencies (>1 s^{-1}), where negligible. Furthermore, at the other end of the co-spectra, they leveled off, revealing that no

low-frequency fluctuations (<0.08 s^{-1}) were contributing to the flux. Thus, for the purpose of this study, the burst lengths (15 min) used in the flux calculations were adequate.

Assessment

Experimental testing of optodes, results, and interpretation of results

Two laboratory tests quantified and compared the responsiveness of optodes and microelectrodes under steady and dynamic oxygen conditions. Two field studies in which we deployed parallel eddy correlation measurements with optodes and microelectrodes investigated the performance of the optode-based eddy correlation instrument under natural riverine and coastal situations.

Laboratory tests

Lab test 1: Response time tests with steady oxygen conditions

The goal of these tests was to determine the response times of the microelectrodes and fast optodes when exposed to sudden changes in oxygen concentration. An optode and microelectrode were mounted next to each other vertically in a micromanipulator, such that their tips were exactly at the same height and less than 2 mm apart. The sensors were connected to their respective electronics (custom analog optode board and custom picoamperemeter), and the signal outputs of the two electronics were recorded on the same data logger at 64 s^{-1}. Before all measurements, optodes and microelectrodes were calibrated using water samples (Salinity S: 35, water temperature T_w: 22°C) purged with nitrogen (0% oxygen saturation) or air (100% air saturation), and the same calibration was repeated at the end of the experiment. (All laboratory measurements reported here used this start/end calibration procedure). For a typical electrode signal reading of 6000 counts, the difference between the oxygen concentration calculated from the beginning and end calibrations, over a period of 10 min, was 2%. For the same count reading by the optodes, the difference in the oxygen concentrations calculated from the beginning and end calibrations was 0.5%, reflecting the small drift of these sensors. The averages of both calibrations were used for the actual calibration of the sensors. The micromanipulator was used to quickly move the sensor tips, initially positioned above one of the calibration fluids, into and out of either one of the two calibration water samples. The 90% response time of the sensors was evaluated by plotting the sensor signal against time. In an additional test, the response time of the Microx TX3 optode system was determined using the same approach. To achieve maximum temporal resolution, the Microx TX3 electronics was operated in "fast sampling" mode, where the instrument updates the analoge signal output every 300 to 400 ms. Between updating events, the analoge output signal is kept constant, thus producing a data record with distinct steps.

Comparison of the sensor signal recordings after the optodes and microelectrodes have been exposed to an abrupt change in oxygen revealed that the response times of both sensors were very similar. This was observed for changes from high to low as well as for changes from low to high oxygen concentrations (Fig. 3). Replicates were made using two different electrodes (5 with the first and 5 with the second) and two different optodes (5 with the first and 6 with the second). The analysis of these records showed that the fast optodes had a 90% response time of 60-240 ms (mean 162 ± 66 ms, n = 11) and the Clark-type microelectrodes of 60-180 ms (mean 160 ± 57 ms, n = 10). These results indicated that the response time of the optode can compete with the response time of the fastest oxygen microelectrode, and that optodes thus may be suitable for eddy correlation measurements. Most of the variability in response time that was observed in both sensors may be attributed to the measuring procedure, i.e., variability associated with the manual lowering of the sensors into the calibration fluid and the diffusive boundary layer forming in the fluid near the surface. The relatively slow lowering of the sensors into the fluid and the diffusive boundary layer both increase the response time, and thus, our response time values should be considered conservative. The fastest recorded response time for the Microx TX3 system was 297 ms or 3.37 s^{-1} (Fig. 3).

The optodes used with the Microx TX3 also had a tapered end but their response was slower (by 146 ms) than that of the custom-built optodes used for the fast oxygen measurements. Though this response time is almost twice as long as those of the microelectrode and the custom-made optode system, it meets the requirements for capturing most of the frequency range of flow and associated oxygen fluctuations measured in aquatic systems so far. These measurements indicate that the high frequency limit is approximately 1 s in high-energy environments and approximately 10 s in low-energy environments (Lorrai et al. 2010). The pre- and post-calibration of the sensors emphasize the advantages associated with the small drift of the optodes. These sensors can be used over extended time periods (hours to days) without a change in their calibration values, whereas electrodes may show a signal drift that varies in magnitude between electrodes and electrode age.

Lab test 2: Response time tests with dynamic oxygen conditions

The goal of these tests was to compare the response times of microelectrodes and fast optodes to oxygen concentrations that rapidly changed over time. A microelectrode and fast optode (read by our custom electronic board) were attached to a holder such that their sensing tips were parallel, at the same height and less than 2 mm apart. The holder with oxygen sensors and an ADV sensor were mounted to a tripod such that sensors and ADV were measuring in the same sampling volume. The sensors then were submerged in a laboratory tank (45 cm wide, 75 cm long, 45 cm deep) filled with sea water (S: 32, T_w: 21.4°C) to a water depth of approximately 40 cm. The sensor volume was positioned at approximately 14 cm above the bottom, i.e., the same position as used in the field measurements.

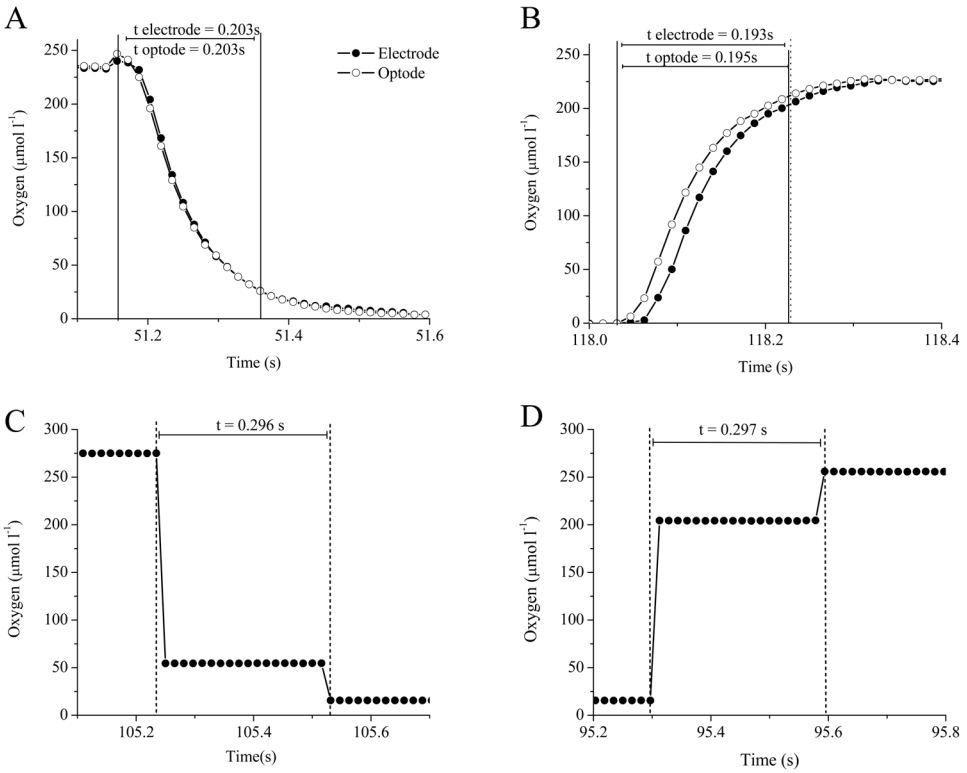

Fig. 3. Response times of oxygen sensors exposed to abrupt changes in oxygen. (A) 90% response time of fast optode and microelectrode when submerged into anoxic solution from air. (B) 90% response time of fast optode and microelectrode when brought from anoxic solution to air. Solid vertical lines indicate start time and 90% response time of the electrode in, and dashed vertical lines indicate start time and 90% response time of the optode. (C) Response time of the Microx TX3 optode system with slower optodes from air to anoxic solution and (D) from anoxic solution to air. Vertical dashed lines indicate start time and 90% response time in C and start time and 100% response time in D (90% response lies between time points). The steps in the analog output signal of the Microx TX3 result from the internal data processing of the Presens instrument.

Flow and oxygen gradients in the tank were established by a gentle flow of nitrogen bubbles, with bubbles emerging from a narrow tube (1.5 mm inner diameter) installed at the bottom of the tank. The opening of the tube was positioned such that the bubbles passed near the sample volume and some bubbles also passed directly through the sample volume. Gas flow was adjusted to produce approximately 2 gas bubbles of approximately 5 mm diameter (measured at the end of the tube) per second. Measurements were recorded at a frequency of 64 s^{-1} and 45 min of data were collected. The performance of the two sensors was evaluated by analyzing the correlation between the two signals.

The comparison of optode and microelectrode performance under rapidly changing oxygen conditions showed that the dynamic response of the optode is comparable to that of the oxygen microelectrode, confirming that the optodes can perform as well as microelectrodes in eddy correlation instruments. For the data recorded in the trough with nitrogen bubble flow (Fig. 4), the correlation coefficient between the oxygen values from the two different sensors was 0.95, and the correlation coefficient between the calculated oxygen fluxes in the experiment reached 0.99. The similar response time of the sensors is reflected in the almost identical recordings of the oxygen fluctuations caused by the bubbles. Comparison of the frequency spectra recorded by both sensors reveal that the oxygen fluctuations were carried mostly by eddies in the 0.0025-3 s^{-1} range, and that both sensors could equally record the concentration changes in the frequency spectrum that were responsible for the fluctuations (Fig. 4A).

Field measurements

Field measurements 1: Wakulla River Site

Our freshwater field site (30.21375N and –84.26175W) was located in the Wakulla River, a clear, spring-fed river located in Wakulla County, Florida (T_w: 22.8°C, S: 0). The river has a depth range of 0.3 to 4 m and is 15 to 61 m wide. At our deployment site, the depth of the river was 3 m and its width approximately 50 m. The site provides relatively constant, unidirectional flow, and the riverbed consists of sand sediments with an average permeability of $2.3 \times 10^{-11} \pm 6.6 \times 10^{-11}$ m^2 and a median grain size of 333 ± 35 µm. During the first measuring campaign at this site, we deployed simultaneously one optode-eddy correlation system with two measuring optodes (one intensity based using the custom build optode board and one lifetime based system using the Microx TX3) and two microelectrode-eddy correlation systems. The two optodes were mounted side by side with a horizontal distance

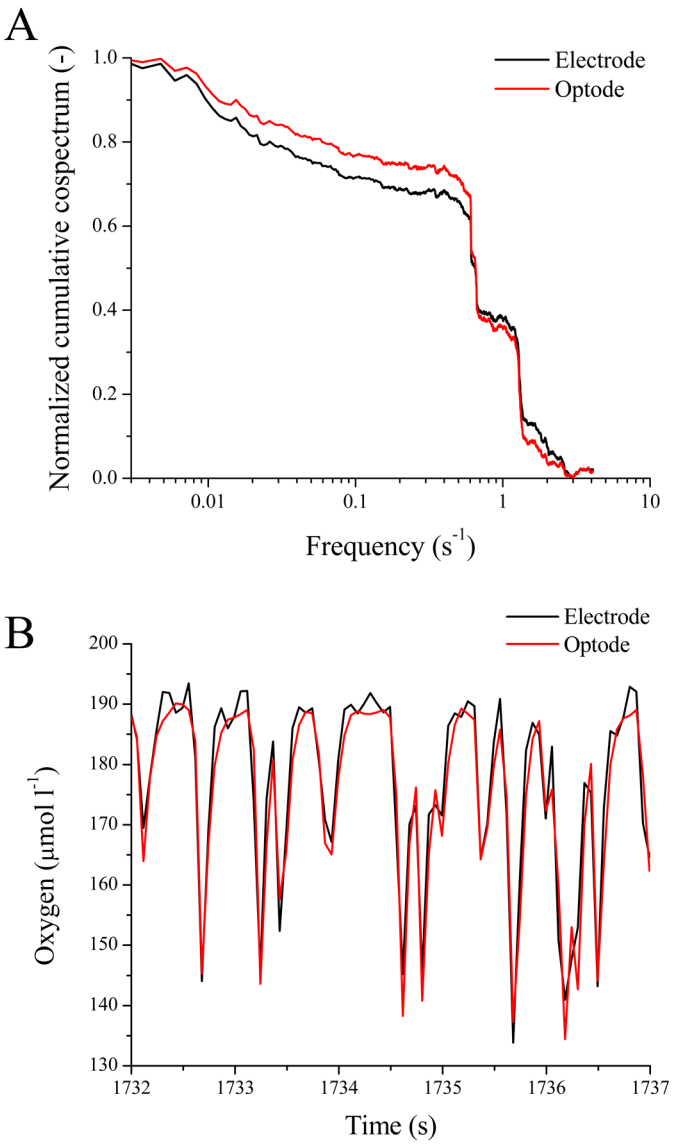

Fig. 4. (A) Normalized cumulative cospectra for electrode and optode, averaged from three 15-min bursts. (B) Correlation of microelectrode and optode oxygen measurements in seawater as it was bubbled with nitrogen gas.

between the sensor tips of 2 cm. The tips were positioned at the vertical edge of the ADV measuring volume. In addition, Hach oxygen sensors were deployed in the water column to measure reference oxygen and temperature values. Average bottom current velocity ranged from 12–25 cm s^{-1} at 14 cm above the sediment. During the measurements, the weather was partly cloudy with no winds or precipitation. The data collected by the Microx TX3 system was corrected to account for the slower response time of the sensor, by shifting the oxygen data forward in time with respect to the velocity data in each measuring burst, until the maximum correlation was achieved (Berg et al. 2003; Lorrai et al. 2010). Though a complete correction is not achievable for this sensor because of its response characteristics, the first-order correction performed here could correct for some of the error caused by slow response time, as seen by the improvement in correlation. The shifting caused a 0.05–9.2% increase in flux, varying with the time interval. The cospectrum of the Microx optode (O2, Fig. 5) shows that the optode did not resolve all of the higher frequencies (i.e., at ~ 0.5 s^{-1}). However these frequencies contributed little to the total flux as demonstrated by the similarity of the average oxygen flux to the fluxes recorded with the other optodes and electrodes (Fig. 6, 7).

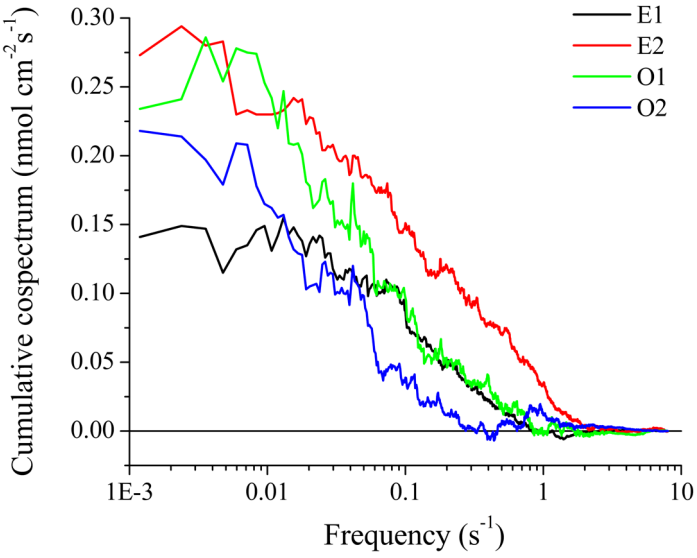

Fig. 5. Cumulative cospectrum from data recorded during the same time interval at the Wakulla River site (black curve: microelectrode 1, E1; red curve: microelectrode 2, E2; green curve: microoptode 1, custom optode/electronics, O1; blue curve: microoptode 2, Microx, O2).

Cospectra and oxygen fluxes calculated from the data recorded by the optode and microelectrode based systems agreed well (Fig. 5, 6) and showed that optodes can be used as sensors for eddy correlation flux measurements in environments with small and fast eddies, as found in this riverine environment.

The flux signal was carried by eddies in the range of ~0.01 to 1 s^{-1}, suggesting that the custom optode and, after frequency correction, the Microx optode, are capable of achieving sufficient temporal resolution for eddy correlation measurements in this environment. During the measuring time interval (12:45 to 14:45 h), the oxygen concentration in the river water increased from 206 ± 14 to 292 ± 12 µmol L^{-1} (average all sensors). Hourly average oxygen fluxes recorded by the two optode-based systems were 195 ± 20 and 152 ± 61 mmol m^{-2} d^{-1} (custom system) and 176 ± 10 and 199 ± 79 mmol m^{-2} d^{-1} (Microx TX3 system) and those recorded by the microelectrode-based systems were 109 ± 52 and 106 ± 38 mmol m^{-2} d^{-1} (electrode 1) and 165.4 ± 59.1 and 126.8 ± 44.1 mmol m^{-2} d^{-1} (electrode 2) (standard deviation, n = 4, positive fluxes indicate upward directed fluxes, Fig. 7).

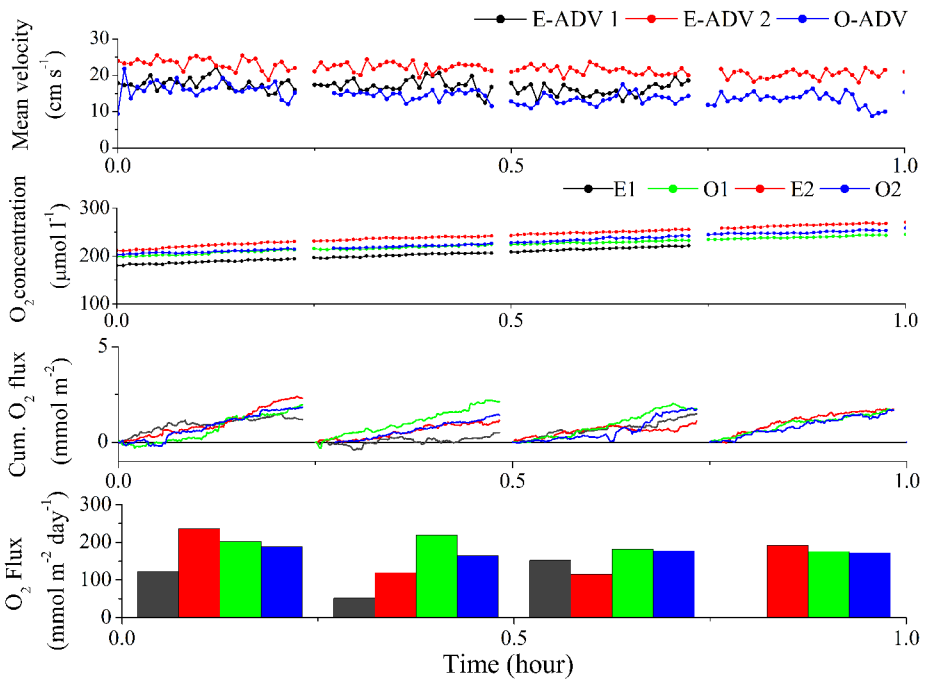

Fig. 6. Data from Wakulla River deployment collected with 2 electrode-eddy systems and 1 optode-eddy system with 2 optodes (black curve/bars: electrode 1, E1; red curve/bars: electrode 2, E2; green curve/bars: optode 1, custom optode/electronics; blue curve/bars: optode 2). Linear detrending was used to derive the oxygen and velocity means used in the flux calculations. (A) 15 min averaged velocity (mean), (B) 15 min averaged oxygen concentration, (C) cumulative oxygen flux over 15 min measuring intervals, (D) 15 min derived calculated oxygen flux of all sensors. Four consecutive 15 min fluxes were averaged together to derive hourly oxygen fluxes. Plant material caught by the electrode 1 tip prevented meaningful measurements of that electrode in the time interval of 0.75–1 h.

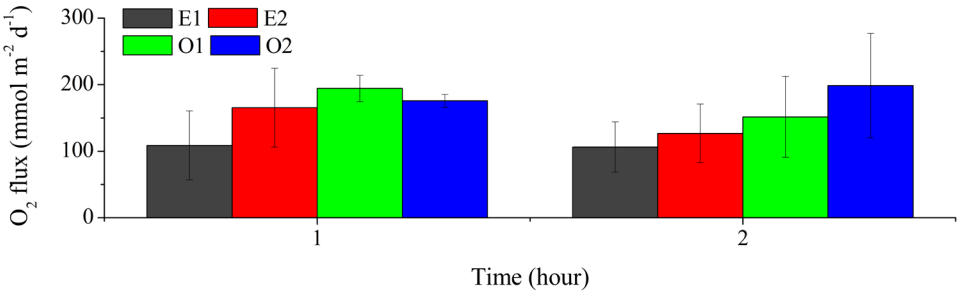

Fig. 7. Hourly oxygen fluxes from the Wakulla River deployment derived from the average of four 15 min bursts recorded by electrode 1 (E1, black bars), electrode 2 (E2, red bars), optode 1 (O1, green bars, custom optode/electronics), and optode 2 (O2, blue bars, MICROX). Linear detrending was used to calculate the mean oxygen and velocity over each bursts, used in the 15 min flux calculations. Error bars represent standard deviation (n = 3 for E1 hour 1, n = 4 for all others).

Natural variation is included in the average fluxes. The difference between optode and microelectrode measured eddy correlation fluxes were statistically not significantly different (paired t test, t = –1.879, p > 0.05, df = 7, n = 8, a calculated average from paired electrode 15 min measurements was used to fill in the one missing electrode flux to get a total of 8 measurements needed for the pair-wise t test).

Field measurements 2: St. Joseph Bay

Our marine field site (29.765333°N, –85.403783°W) was located in St. Joseph Bay, on the Gulf coast of Florida. This well-protected bay is bounded on three sides with the mainland to the east, Cape San Blas to the south, and the St. Joe Peninsula to the west. The upper 20 cm of the sediment at this site consists of well-sorted quartz sand with an average permeability of $4.43 \times 10^{-11} \pm 4.13 \times 10^{-13}$ m^2. The optode-based eddy correlation system and microelectrode-based eddy correlation system were mounted onto the same frame and simultaneously deployed at about 1 m water depth (T_w: 9.9°C, S: 32.7). The sensors were positioned so that the measuring tips of both sensors were in the same measuring volume. The ADV

measuring volume was positioned at 14 cm above the sediment, and the measurements showed average bottom current velocities of 0.15–2.26 cm s^{-1} at this depth. An Aandrea Seaguard probe recorded oxygen and temperature reference values near the eddy instrument.

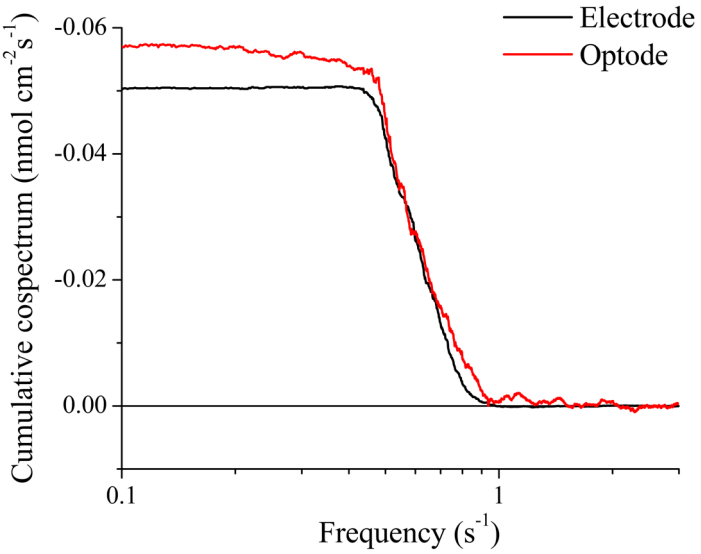

Fig. 8. Cumulative copectra from the electrode and optode for the same time interval at the St. Joe Bay deployment.

The cumulative cospectra for the two sensors showed that frequencies in the range of 0.4 –1 s^{-1} carried the majority of the flux signal (Fig. 8), suggesting that surface waves were a dominant factor affecting the flux measurements. The close agreement of the cospectra measured in the same measuring volume shows that both sensors were equally capable of picking up the frequencies contributing to the flux, and the cumulative oxygen flux records showed a good agreement between the two sensors (Fig. 9).

During the 13 h deployment, the mean oxygen concentrations ranged from 288 to 346 µmol L^{-1}, as measured by the microelectrode and from 287 to 359 µmol L^{-1}, measured by the optode. The hourly fluxes recorded by the optode-based eddy correlation instrument ranged from –70 ± 28 to –12 ± 6 mmol m^{-2} d^{-1} and the fluxes measured by the microelectrode based system from –59 ± 25 to 19 ± 1 mmol m^{-2} d^{-1} (Fig. 10). The average fluxes measured by the two systems were statistically not different (paired *t* test, $t = 0.888$, $P > 0.05$, df = 10, $n = 13$).

Discussion

Response time

Fast sensor response is a crucial criterion for successful eddy correlation measurements. The sensor must be fast enough to resolve the turbulent fluctuations of the water carrying the oxygen flux and small enough to not interfere with the water flow. The shortest time scales of eddies significantly contributing to

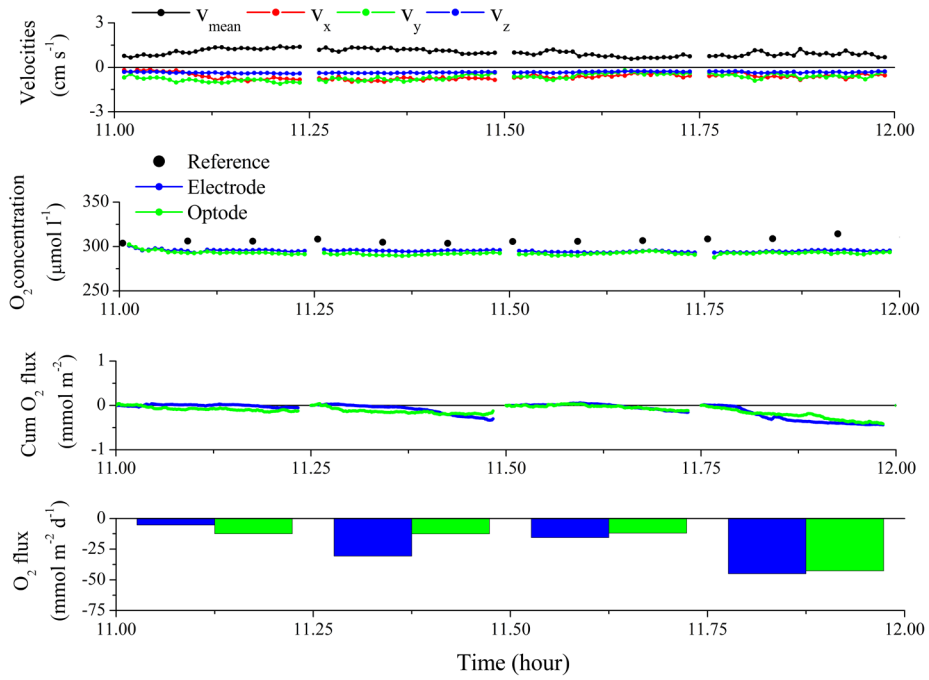

Fig. 9. Optode (green curves and bars, custom optode and electronics) and microelectrode (blue curves and bars) data from the St. Joe Bay deployment over four 15 min measuring bursts. Linear detrending was used to derive the oxygen and velocity means over individual bursts, used in the 15 min flux calculations. (A) 15 min averaged velocity (x,y,z, and mean) from the ADV used for the velocity measurements, (B) 15 min averaged oxygen concentrations for the electrode and optode, (C) cumulative oxygen flux over 15 min data intervals, (D) mean oxygen flux of these 15 min intervals. Negative fluxes indicate oxygen consumption or flux into the sediment. Measurements were taken after sundown.

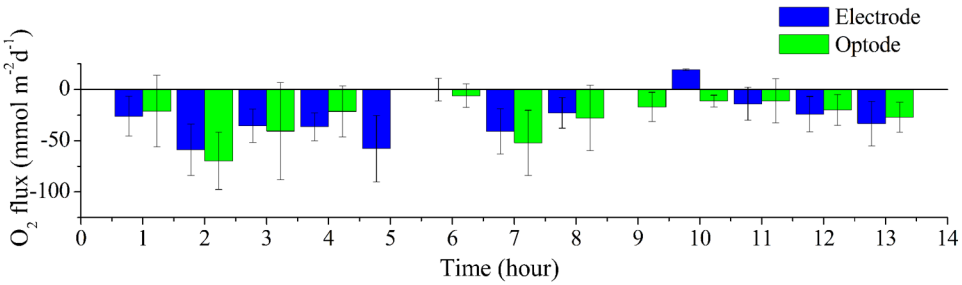

Fig. 10. Hourly oxygen fluxes over the entire measuring period during the deployment at St. Joe Bay derived from averaging of 4 consecutive 15 min fluxes collected by the electrode-based system (blue bars) and optode-based system (green bars). Linear detrending was used to derive the oxygen and velocity means over the 15 min bursts used in the flux calculations. One hourly interval from the optode measurements was removed at 5 h, and one from the electrode measurements at 9 h due to excessive noise in the sensor signals.

the flux in high-energy environments is 1 s (Lorrai et al. 2010). The frequency of eddies measured at our field sites ranged from approximately 0.01–2 s^{-1} at our freshwater river site and from 0.4–1 s^{-1} at our marine site. With 2 to 3 s^{-1} maximum sampling rate, the Microx TX3 system thus operates at the limit of the required temporal resolution, however, the field deployments indicated that the Microx TX3 system can be used for eddy correlation measurements with the application of a frequency response correction. For sensors that are too slow to capture the high frequency fluctuations of oxygen (>1 s^{-1}), such frequency response corrections may be used to achieve a higher reliability of the flux calculations (Eugster and Senn 1995; Horst 1997; Horst 2000). For some of the measuring intervals at the Wakulla river deployment, the frequency shift correction applied to the data collected by the slower Presens sensor resulted in fluxes that were 0.1% to 9% larger than the original data. The laboratory tests revealed that the optimized microelectrodes and optodes respond equally fast to changes in oxygen concentration. The equal performance of optode and microelectrode is supported by the similarity of the cumulative cospectra of the sensors, which show that optode and microelectrode identified eddies in the same frequency ranges as main contributors to the flux signal. The cumulative cospectra from lab test 2 (Fig. 4A) and the St. Joe Bay deployment (Fig. 8), in which the sensors were mounted side by side in the same measuring volume, were tightly correlated, whereas those from the Wakulla river deployment have more variation. This larger difference between the two systems was caused by the spatial separation of the microelectrode and optode eddy correlation instruments during the Wakulla river deployment. Although we chose a relatively homogeneous environment for these comparisons (river bed with sandy sediment and unidirectional flow) and were measuring at the same time with the instruments only 10 m horizontally apart, some natural variation caused by small differences in flow structure and sediment chemical and biological characteristics between sites is expected.

Performance of microelectrode and optode during field tests

The linear trends seen in the cumulative fluxes from the Wakulla River and St. Joe Bay data sets reflect consistent strong flux signals over the interrogated time periods and indicate a statistically good representation of all eddy sizes that contributed to the flux (Berg et al. 2009). Cumulative fluxes from all sensors showed this linear trend, supporting our hypothesis that optodes can perform equally well in aquatic eddy correlation measurements as microelectrodes. This conclusion is strengthened by the high correlation coefficients of instantaneous oxygen concentration (0.92 at Wakulla and 0.97 at St. Joe) between the two sensor types operating in dynamic environments. Because there is natural variation due to the spatial separation of the sensors, we consider this correlation to be very good, underlining that both systems operated equally well in measuring the oxygen fluxes.

Optode and microelectrode sensor technology

Optode advantages include virtually no signal drift when used with internal referencing or in fluorescence lifetime mode (Klimant et al. 1995; Klimant et al 1997; Wenzhöfer et al. 2001), no stirring sensitivity as they don't consume oxygen, relatively simple design and construction, and ruggedness. This has enabled in situ applications (Glud et al. 1999; Wenzhöfer et al 2000). This study documents that optodes are a viable alternative to microelectrode-based eddy correlation measurements. This may become even more apparent in the coming years, where new highly sensitive and fast sensing material and measuring instruments emerge. For instance, taking advantage of highly sensitive chemistries (i.e., platinum (II)octaethylporphyrin –PtOEP) in combination with antenna pigments (i.e., Cumarion–Macrolex fluorescence yellow) that ensure very efficient energy transfer, extremely thin O_2 sensor layers of a few microns can be applied to optode tips (Mayr et al. 2009). Such work is in progress and will further improve sensor performance and response time. Lifetime-based optode measurements are not affected by variations in ambient light nor are they susceptible to electronic drift (Holst et al. 1995a, 1995b, 1998; Liebsch et al. 2000).

Comments and recommendations

This study shows that existing technology makes the oxygen optode a suitable sensor for eddy correlation measurements in aquatic environments. The results from the

riverine system with unidirectional flow and the coastal system with oscillating flow show that the optodes perform well in either system. The present custom-built system could be improved by compacting the electronics into a smaller housing that could be placed closer to the measuring volume, thereby reducing signal noise. Our instrument was designed for deployments in the shallow shelf environment with a pressure rating of 300 m. By using underwater housings with higher pressure ratings and deep sea fiber optic cables, the instrument could be adapted to full ocean depths. In addition to the insensitivity to flow and the lack of signal drift, the advantage of the optode-based system is the simpler, and thus less expensive, sensor that also can be repaired, in contrast to the microelectrodes. As the sensor is fully exposed during measurements, this advantage gains importance when deploying eddy correlation instruments in coastal and shelf environments, where bottom currents are relatively strong, fish and benthic organisms are abundant, and particle loads in the boundary currents are high. These environmental characteristics put the fragile sensors at a high risk of breaking and an easily replaceable, inexpensive sensor thus presents a significant advantage when conducting extensive measurement campaigns. Biofouling is a common problem when deploying sensors in aquatic environments, and using optodes can reduce this problem through addition of antibiotics to the indicator dye. Future development of optodes for other solutes may adapt the eddy correlation technique for the measurement of a variety of environmentally important solutes.

References

Berg, P., H. Roy, F. Janssen, V. Meyer, B. Jorgensen, M. Huettel, and D. de Beer. 2003. Oxygen uptake by aquatic sediments measured with a novel non-invasive eddy-correlation technique. Mar. Ecol. Progr. Ser. 261:75-83 [doi:10.3354/meps261075].

———, H. Roy, and P. L. Wiberg. 2007. Eddy correlation flux measurements: The sediment surface area that contributes to the flux. Limnol. Oceanogr. 52:1672-1684 [doi:10.4319/lo.2007.52.4.1672].

———, and M. Huettel. 2008. Monitoring the seafloor using the noninvasive eddy correlation technique: integrated benthic exchange dynamics. Oceanography 21:164-167 [doi:10.5670/oceanog.2008.13].

———, R. N. Glud, A. Hume, H. Stahl, O. Kazumasa, V. Meyer, and H. Kitazato. 2009. Eddy correlation measurements of oxygen uptake in deep ocean sediments. Limnol. Oceanogr. Methods 7:576-584 [doi:10.4319/lom.2009.7.576].

Brand, A., D. F. Mcginnis, B. Wehrli, and A. Wueest. 2008. Intermittent oxygen flux from the interior into the bottom boundary of lakes as observed by eddy correlation. Limnol. Oceanogr. 53:1997-2006 [doi:10.4319/lo.2008.53.5.1997].

Cahoon, L. B. 1999. The role of benthic microalgae in neritic ecosystems. Oceanogr. Mar. Biol. 37:47-86.

Canfield, D. E., and others. 1993. Pathways of organic carbon oxidation in three continental margin sediments. Mar. Geol. 113:27-40 [doi:10.1016/0025-3227(93)90147-N].

Eugster, W., and W. Senn. 1995. A cospectral correction model for measurement of turbulent NO_2 flux. Bound. Layer Meteorol. 74:321-340 [doi:10.1007/BF00712375].

Glud, R. N. 2008. Oxygen dynamics of marine sediments. Mar. Biol. Res. 4:243-289 [doi:10.1080/17451000801888726].

———, N. B. Ramsing, J. K. Gundersen, and I. Klimant. 1996. Planar optodes, a new tool for fine scale measurements of two-dimensional O_2 distribution in benthic communities. Mar. Ecol. Prog. Ser. 140:217-226 [doi:10.3354/meps140217].

———, I. Klimant, G. Holst, V. Meyer, M. Kuhl, and J. K. Gundersen. 1999. Adaptation, test and in situ measurements with O-2 microopt(r)odes on benthic landers. Deep Sea Res. I 46:171-183 [doi:10.1016/S0967-0637(98)00068-5].

———, P. Berg, A. Hume, P. Batty, M. E. Blicher, K. Lennert, and S. Rysgaard. 2010. Benthic O_2 exchange across hard-bottom substrates quantified by eddy correlation in a sub-Arctic fjord. Mar. Ecol. Progr. Ser. 417:1-12 [doi:10.3354/meps08795].

Grattan, L. S., and B. T. Meggitt [eds.]. 2010. Optical fiber sensor technology: Vol. 4: Chemical and environmental sensing (Optoelectronics, imaging and sensing), 1st ed. Springer.

Gruber, W. R., I. Klimant, and O. S. Wolfbeis. 1993. Instrumentaion for optical measurement of dissolved-oxygen based on solid-state technology. Proc. Adv. Fluoresc. Sens. Technol. 1885:448-457.

Gundersen, J. K., N. B. Ramsing, and R. N. Glud. 1998. Predicting the signal of O-2 microsensors from physical dimensions, temperature, salinity, and O-2 concentration. Limnol. Oceanogr. 43:1932-1937.

Holst, G. A., M. Kuehl, and I. Klimant. 1995a. A novel measuring system for oxygen microoptodes based on a phase modulation technique, p. 1-12. Proc. SPIE 2508, 387 (1995); [doi:10.1117/12.221754].

———, T. Koester, E. Voges, and D. W. Luebbers. 1995b. FLOX—an oxygen-flux-measuring system using a phase-modulation method to evaluate the oxygen-dependent fluorescence lifetime. Sens. Actuators 29:231-239 [doi:10.1016/0925-4005(95)01688-0].

———, R. N. Glud, M. Kuhl, and I. Klimant. 1997. A microoptode array for fine-scale measurement of oxygen distribution. Sens. Actuat. B Chem. 38:122-129 [doi:10.1016/S0925-4005(97)80181-5].

———, O. Kohls, I. Klimant, B. Koenig, M. Kuehl, and T. Richter. 1998. A modular luminescence lifetime imaging system for mapping oxygen distribution in biological samples. Sens. Actuators B 51:163-170 [doi:10.1016/S0925-4005(98)00232-9].

Horst, T. W. 1997. A simple formula for attenuation of eddy fluxes measured with first-order-response scalar sensors. Bound. Layer Meteorol. 82:219-233 [doi:10.1023/A:1000229130034].

———. 2000. On frequency response corrections for eddy covariance flux measurements. Bound. Layer Meteorol. 94:517-520 [doi:10.1023/A:1002427517744].

———, and D. H. Lenschow. 2009. Attenuation of scalar fluxes measured with spatially-displaced sensors. Bound. Layer Meteorol. 130:275-300 [doi:10.1007/s10546-008-9348-0].

Hume, A. C., P. Berg, and K. J. McGlathery. 2011. Dissolved oxygen fluxes and ecosystem metabolism in an eelgrass (*Zostera marina*) meadow measured with the eddy correlation technique. Limnol. Oceanogr. 56:86-96 [doi:10.4319/lo.2011.56.1.0086].

Jahnke, R. A. 1996. The global ocean flux of particulate organic carbon - areal distribution and magnitude. Glob. Biogeochem. Cycles 10:71-88 [doi:10.1029/95GB03525].

———, and D. B. Craven. 1995. Quantifying the role of heterotrophic bacteria in the carbon cycle—a need for respiration rate measurements. Limnol. Oceanogr. 40:436-441 [doi:10.4319/lo.1995.40.2.0436].

Kautsky, H. 1939. Quenching of luminescence by oxygen. Trans. Faraday Soc. 35:0216-0218.

Klimant, I., V. Meyer, and M. Kuehl. 1995. Fiber-optic oxygen microsensors, a new tool in aquatic biology. Limnol. Oceanogr. 40:1159-1165 [doi:10.4319/lo.1995.40.6.1159].

———, M. Kuhl, R. N. Glud, and G. Holst. 1997. Optical measurements of oxygen and other environmental parameters in microscale: Strategies and biological applications. Sens. Actuators B 38-39:29-27 [doi:10.1016/S0925-4005(97)80168-2].

Kuwae, T., K. Kamio, T. Inoue, E. Miyoshi, and Y. Uchiyama. 2006. Oxygen exchange flux between sediment and water in an intertidal sandflat, measured in situ by the eddy-correlation method. Mar. Ecol. Progr. Ser. 307:59-68 [doi:10.3354/meps307059].

Lee, X., W. J. Massman, and B. E. Law. 2004. Handbook of micrometeorology: a guide for surface flux measurement and analysis. Kluwer Academic.

Liebsch, G., I. Klimant, B. Frank, G. Holst, and O. S. Wolfbeis. 2000. Luminescence lifetime imaging of oxygen, pH, and carbon dioxide distribution using optical sensors. Appl. Spectrosc. 54:548-559 [doi:10.1366/0003702001949726].

Lorrai, C., D. F. Mcginnis, P. Berg, A. Brand, and A. Wuest. 2010. Application of oxygen eddy correlation in aquatic systems. J. Atmos. Ocean. Technol. 27:1533-1546 [doi:10.1175/2010JTECHO723.1].

McGinnis, D. F., P. Berg, A. Brand, C. Lorrai, T. J. Edmonds, and A. Wuest. 2008. Measurements of eddy correlation oxygen fluxes in shallow freshwaters: Towards routine applications and analysis. Geophys. Res. Lett. 35:L04403.

Mayr, T., and others. 2009. Light harvesting as a simple and versatile way to enhance brightness of luminescent sensors. Anal. Chem. 81:6541-6545 [doi:10.1021/ac900662x].

Reimers, C. E., T. Özkan-Haller, P. Berg, A. Devol, K. Mccann-Grosvenor, and R. D. Sanders. 2012. Benthic oxygen consumption rates during hypoxic conditions on the Oregon continental shelf: Evaluation of the eddy correlation method. J. Geophys. Res. 117:C02021, 1-18 [doi:10.1029/2011JC007564].

Revsbech, N. P. 1989. An oxygen microsensor with guard cathode. Limnol. Oceanogr. 34:474-478 [doi:10.4319/lo.1989.34.2.0474].

———, B. B. Jørgensen, and T. H. Blackburn. 1979. Oxygen in the sea bottom measured with a microelectrode. Science 207:1355-1356.

———, J. Sorensen, T. H. Blackburn, and J. P. Lomholt. 1980. Distribution of oxygen in marine sediments measured with microelectrodes. Limnol. Oceanogr. 25(N3):403-411 [doi.org/10.4319/lo.1980.25.3.0403].

———, and D. M. Ward. 1983. Oxygen microelectrode that is sensitive to medium chemical composition: Use in an acid microbial mat dominated by *Cyanidium caldarium*. Appl. Environ. Microbiol. 45:755-759.

———, and B. B. Jørgensen. 1986. Microelectrodes: their use in microbial ecology, p. 293-352. *In* K. C. Marshall [ed.], Advances in microbial ecology. Plenum Press.

Reynolds, O. 1895. On the dynamical theory of incompressible viscous fluids and the determination of the criterion. Phil. Trans. R. Soc. Lond. A Math. Phys. Sci. 186:123-164.

Smith, S. W. 1997. The scientist and engineer's guide to digital signal processing. California Technical Publishing.

Stern, O., and M. Volmer. 1919. Über die Abklingzeit der Fluoreszenz. Physikalische Zeitschrift 20:183-188.

Swinbank, W. C. 1951. The measurement of vertical transer of heat and water vapor by eddies in the lower atmosphere. J. Meteorol. 8:135-146 [doi:10.1175/1520-0469(1951)008<0135:TMOVTO>2.0.CO;2].

Wenzhöfer, F., O. Holby, R. N. Glud, H. K. Nielsen, and J. K. Gundersen. 2000. In situ microsensor studies of a hydrothermal vent at Milos, Greece. Mar. Chem. 69:43-54 [doi:10.1016/S0304-4203(99)00091-2].

———, O. Holby, and O. Kohls. 2001. Deep penetrating benthic oxygen profiles measured in situ by oxygen optodes. Deep Sea Res. I 48:1741-1755 [doi:10.1016/S0967-0637(00)00108-4].

Ziebis, W., M. Huettel, and S. Forster. 1996. Impact of biogenic sediment topography on oxygen fluxes in permeable seabeds. Mar. Ecol. Progr. Ser. 140:227-237 [doi:10.3354/meps140227].

Submitted 10 August 2011
Revised17 February 2012
Accepted 12 March 2012